



Brazilian Journal of Physics

ISSN: 0103-9733

luizno.bjp@gmail.com

Sociedade Brasileira de Física  
Brasil

Ferreira, Erasmo; Baltar, Vera L.  
Roles of Wave Functions in the Electroproduction of Vector Mesons  
Brazilian Journal of Physics, vol. 37, núm. 2B, june, 2007, pp. 532-537  
Sociedade Brasileira de Física  
São Paulo, Brasil

Available in: <http://www.redalyc.org/articulo.oa?id=46437410>

- How to cite
- Complete issue
- More information about this article
- Journal's homepage in redalyc.org

redalyc.org

Scientific Information System  
Network of Scientific Journals from Latin America, the Caribbean, Spain and Portugal  
Non-profit academic project, developed under the open access initiative

## Roles of Wave Functions in the Electroproduction of Vector Mesons

Erasmio Ferreira

*Instituto de Física, Universidade Federal do Rio de Janeiro  
C.P. 68528, Rio de Janeiro 21945-970, RJ, Brazil*

and Vera L. Baltar

*Departamento de Física, Pontifícia Universidade Católica do Rio de Janeiro  
C.P. 38071, Rio de Janeiro 22452-970, RJ, Brazil*

Received on 7 November, 2006

Elastic vector meson electroproduction is calculated through integrals of the overlap product of photon and vector meson wave functions, multiplied by the amplitude for the scattering of  $q\bar{q}$  dipole pairs off the proton. In this nonperturbative QCD calculation, for sizes of the overlap functions that are smaller than the typical ranges of the interaction of the dipoles with the proton, the amplitudes factorize, with overlap strengths (integration extended over the light front coordinates describing the  $q\bar{q}$  dipoles) containing all  $Q^2$  dependence of the observables. This factorization is important in the description of the experimental data for all S-wave vector mesons.

Keywords: Electroproduction; Vector mesons; Wave functions; Nonperturbative QCD; Stochastic vacuum model; Mesons

### I. INTRODUCTION

In nonperturbative treatments of elastic photo and electroproduction of vector mesons [1–3] the photon and vector meson wave functions appear as explicit ingredients of the calculation, with an overlap product formed to describe the transition from real or virtual photon to the final meson state. The photon and vector meson are treated in a simple dipole model of quark-antiquark distribution functions, which is responsible for the hadronic character of the interaction with the proton. On the other side of the process, the proton is also treated as a system of three quarks (or a system  $q\bar{q}$  in a diquark model structure). The transition from photon to meson and the interaction with the proton occurs in the presence of a background QCD field. The Stochastic Vacuum Model [4, 5] gives a framework for this calculation and has been used with success in the study of  $J/\psi$  photo- and electroproduction processes. The calculation requires no new free parameters, incorporating the knowledge acquired in applications of hadron-hadron scattering [6], based on a functional approach [7].

These successful results give basis and justification for a practical use of simple dipole wave functions of photons and mesons and for the purely nonperturbative treatment of elastic and single diffractive vector meson ( $\rho, \omega, \phi, \psi, \Upsilon$ )

The treatment of  $J/\psi$  electroproduction exhibits clearly the factorization property [3], with all  $Q^2$  dependence of the amplitudes and cross sections contained in the strength of the overlap of virtual photon and meson wave functions. The overlap strength is defined as the integral of the overlap product of wave functions, weighted with  $r^2$  ( $r$  is the dipole separation), over the light-cone coordinates of the  $q\bar{q}$  dipole [8].

This factorization property of the amplitude is favoured by the small size of the overlap function, which in the heavy vector meson  $J/\psi$  case is smaller than the typical range (the correlation length of the nonperturbative QCD vacuum) of the interaction with the proton. For light vector mesons, this con-

dition occurs in electroproduction as the photon virtuality  $Q^2$  increases.

In view of the importance of this analysis for the interpretation and description of the experimental information on vector meson production, we study in this paper the properties of the photon-meson overlaps and overlap strengths for different vector mesons.

The description of the energy dependence requires a specific model for the coupling of  $q\bar{q}$  dipoles to the proton. In previous nonperturbative calculations of photo and electroproduction of  $J/\psi$  mesons [1–3], where a quantitative description of all experimental data was envisaged, the two-pomeron model of Donnachie and Landshoff [9] was successfully employed. All QCD and hadronic parameters used in our calculation have been defined before [10]. In perturbative approaches the energy dependence is taken into account through the gluon distributions in the proton [11–14].

We introduce light cone wave functions and describe their overlaps, comparing results for the  $\rho, \omega, \phi, J/\psi$  and  $\Upsilon$  mesons.

### Basic formulae and Ingredients

We first some basic formulae developed in our previous work on photo- and electro- production [1–3], where details can be found.

The amplitude for electroproduction of a vector meson  $V$  in polarization state  $\lambda$  is written in our framework

$$T_{\gamma^* p \rightarrow V, \lambda}(s, t; Q^2) = \int d^2\mathbf{R}_1 dz_1 \rho_{\gamma^* V, \lambda}(Q^2; z_1, \mathbf{R}_1) J(s, \mathbf{q}, z_1, \mathbf{R}_1), \quad (1)$$

$$J(s, \mathbf{q}, z_1, \mathbf{R}_1) = \int d^2\mathbf{R}_2 d^2\mathbf{b} e^{-i\mathbf{q} \cdot \mathbf{b}} |\psi_p(\mathbf{R}_2)|^2 S(s, b, z_1, \mathbf{R}_1, z_2 = 1/2, \mathbf{R}_2). \quad (2)$$

Here

$$\rho_{\gamma^* V, \lambda}(Q^2; z_1, \mathbf{R}_1) = \psi_{V\lambda}(z_1, \mathbf{R}_1)^* \psi_{\gamma^*\lambda}(Q^2; z_1, \mathbf{R}_1) \quad (3)$$

represents the overlap of virtual photon (virtuality  $Q^2$ ) and vector meson wave functions, and  $S(s, b, z_1, \mathbf{R}_1, 1/2, \mathbf{R}_2)$  is the scattering amplitude of two dipoles with separation vectors  $\mathbf{R}_1, \mathbf{R}_2$ , colliding with impact parameter vector  $\vec{b}$ ;  $\vec{q}$  is the momentum transfer.

The form of overlap written in eq.(3) corresponds to SCHC (s-channel helicity conservation); generalizations can be made introducing a matrix in the polarization indices. For the proton structure we adopt a simple diquark model.

The construction of the wave functions is made in a reference frame where the vector meson is essentially at rest, and we therefore use light-cone coordinates [15–20]. The degrees of freedom for the dipole pair are the  $q \rightarrow \bar{q}$  vector in the transverse plane  $\mathbf{r} = (r \cos \theta, r \sin \theta)$ , and the momentum fractions  $z$  of the quark and  $\bar{z} = (1 - z)$  of the antiquark.

### Photon wave functions

The  $q\bar{q}$  wave function of the photon carries as labels the virtuality  $Q^2$  and the polarization state  $\lambda$ . The  $q\bar{q}$  state is in a configuration with given flavour ( $f, \bar{f}$ ) and helicities ( $h, \bar{h}$ ). The colour part of the wave function leads to an overall multiplicative factor  $\sqrt{N_c}$ . The helicity and spatial configuration part of  $\Psi_{\gamma^*, \lambda}(Q^2; z, r, \theta)$  is calculated in light-cone perturbation theory. The photon couples to the electric charge of the quark-antiquark pair with  $e_f \delta_{f\bar{f}}$ , where  $e_f = \hat{e}_f \sqrt{4\pi\alpha}$  and  $\hat{e}_f$  is the quark charge in units of the elementary charge for each flavour. In lowest order perturbation theory, for each polarization  $\lambda$  and flavour  $f$  content, we write [1–3, 11, 16, 21],

$$\Psi_{\gamma^*, +1}(Q^2; z, r, \theta) = \hat{e}_f \frac{\sqrt{6\alpha}}{2\pi} \left[ i\epsilon_f e^{i\theta} (z\delta_{h,+}\delta_{\bar{h},-} - \bar{z}\delta_{h,-}\delta_{\bar{h},+}) K_1(\epsilon_f r) + m_f \delta_{h,+}\delta_{\bar{h},+} K_0(\epsilon_f r) \right], \quad (4)$$

$$\Psi_{\gamma^*, -1}(Q^2; z, r, \theta) = \hat{e}_f \frac{\sqrt{6\alpha}}{2\pi} \left[ i\epsilon_f e^{-i\theta} (\bar{z}\delta_{h,+}\delta_{\bar{h},-} - z\delta_{h,-}\delta_{\bar{h},+}) K_1(\epsilon_f r) + m_f \delta_{h,-}\delta_{\bar{h},-} K_0(\epsilon_f r) \right] \quad (5)$$

$$\Psi_{\gamma^*, 0}(Q^2; z, r) = \hat{e}_f \frac{\sqrt{3\alpha}}{2\pi} (-2z\bar{z}) \delta_{h,-\bar{h}} Q K_0(\epsilon_f r), \quad (6)$$

where

$$\epsilon_f = \sqrt{z(1-z)Q^2 + m_f^2}, \quad (7)$$

$\alpha = 1/137.036$ ,  $m_f$  is the current quark mass (the values in this presentation are  $m_u = m_d = 0.2$ ,  $m_s = 0.3$ ,  $m_c = 1.25$  and  $m_b = 4.2$  GeV).

### Vector meson wave functions

The flavour dependence of the  $\rho(770)$ ,  $\omega(782)$ ,  $\phi(1020)$ ,  $J/\psi(1S)$  and  $\Upsilon(1S)$  mesons are, respectively,  $(u\bar{u} - d\bar{d})/\sqrt{2}$  (isospin 1),  $(u\bar{u} + d\bar{d})/\sqrt{2}$  (isospin 0),  $s\bar{s}$ ,  $c\bar{c}$

and  $b\bar{b}$ . We take the spin structure determined by the vector current, with expressions similar to those of the photon [1, 2, 21, 22]. We thus write

$$\begin{aligned} \Psi_{V,+1}(z, r, \theta) &= \left( -ie^{i\theta} \partial_r (z\delta_{h,+}\delta_{\bar{h},-} - \bar{z}\delta_{h,-}\delta_{\bar{h},+}) \right. \\ &\quad \left. + m_f \delta_{h,+}\delta_{\bar{h},+} \right) \phi_V(z, r), \\ \Psi_{V,-1}(z, r, \theta) &= \left( -ie^{-i\theta} \partial_r (\bar{z}\delta_{h,+}\delta_{\bar{h},-} - z\delta_{h,-}\delta_{\bar{h},+}) \right. \\ &\quad \left. + m_f \delta_{h,-}\delta_{\bar{h},-} \right) \phi_V(z, r), \end{aligned} \quad (8)$$

$$\Psi_{V,0}(z, r) = \left( \omega 4z\bar{z}\delta_{h,-\bar{h}} \right) \phi_V(z, r). \quad (9)$$

Here  $\lambda = \pm 1$  and 0 denote transverse and longitudinal polarizations of the vector meson,  $h$  and  $\bar{h}$  represent the helicities of quark and antiquark respectively and  $m_f$  is the quark current mass. The scalar function  $\phi_V(z, r)$  contains two parameters,  $N$  and  $\omega$ , which have different values for transverse and longitudinal states; they are determined by the normalization condition and the leptonic decay width [1–3]. The parameter  $\omega$  controls the size of the hadron.

We consider two forms for  $\phi_V(z, r)$ . One is based on the relativistic equation for two particles confined by an oscillator potential and is written

$$\phi_{BSW}(z, r) = \frac{N\sqrt{z\bar{z}}}{\sqrt{4\pi}} \exp\left[-\frac{M_V^2}{2\omega^2}(z - \frac{1}{2})^2\right] \exp\left[-\frac{\omega^2 r^2}{2}\right], \quad (10)$$

which corresponds to the Bauer-Stech-Wirbel (BSW) prescription [23]. Here  $M_V$  represents the vector meson mass.

The second form follows the Brodsky-Lepage (BL) prescription [18, 20] for the construction of a light-cone wave function from a non-relativistic one is written

$$\phi_{BL}(z, r) = \frac{N}{\sqrt{4\pi}} \exp\left[-\frac{m_f^2(z - \frac{1}{2})^2}{2z\bar{z}\omega^2}\right] \exp[-2z\bar{z}\omega^2 r^2]. \quad (11)$$

The input experimental data for the S-wave vector mesons [24] are shown in Table I and the derived wave function parameters  $\omega$  and  $N$  are given in Table II.

TABLE I: S-wave vector meson data. The coupling  $f_V$  and the decay width  $\Gamma_{e^+e^-}$  are related through  $f_V^2 = (3M_V\Gamma_{e^+e^-})/(4\pi\alpha^2)$ . The quantity  $\hat{e}_V$  is the effective quark charge in units of the elementary charge, determined by the  $q\bar{q}$  structure.

Meson	$M_V(\text{MeV})$	$\hat{e}_V$	$\Gamma_{e^+e^-}(\text{keV})$	$f_V(\text{GeV})$
$\rho(770)$	$775.9 \pm 0.5$	$1/\sqrt{2}$	$6.77 \pm 0.32$	$0.15346 \pm 0.0037$
$\omega(782)$	$782.57 \pm 0.12$	$1/3\sqrt{2}$	$0.60 \pm 0.02$	$0.04588 \pm 0.0008$
$\phi(1020)$	$1019.456 \pm 0.02$	$-1/3$	$1.261 \pm 0.03$	$0.07592 \pm 0.0018$
$J/\psi(1S)$	$3096.87 \pm 0.04$	$2/3$	$5.14 \pm 0.31$	$0.26714 \pm 0.0081$
$\Upsilon(1S)$	$9460.30 \pm 0.26$	$-1/3$	$1.314 \pm 0.029$	$0.23607 \pm 0.0026$

TABLE II: Parameters of the vector meson wave functions

	BSW			
	transverse		longitudinal	
	$\omega(\text{GeV})$	$N$	$\omega(\text{GeV})$	$N$
$\rho$	0.2159	5.2082	0.3318	4.4794
$\omega$	0.2084	5.1770	0.3033	4.5451
$\phi$	0.2568	4.6315	0.3549	4.6153
$J/\psi$	0.5770	3.1574	0.6759	5.1395
$\Upsilon$	1.2850	2.4821	1.3582	5.9416

	BL			
	transverse		longitudinal	
	$\omega(\text{GeV})$	$N$	$\omega(\text{GeV})$	$N$
$\rho$	0.2778	2.0766	0.3434	1.8399
$\omega$	0.2618	2.0469	0.3088	1.8605
$\phi$	0.3113	1.9189	0.3642	1.9201
$J/\psi$	0.6299	1.4599	0.6980	2.3002
$\Upsilon$	1.3250	1.1781	1.3742	2.7779

### Overlap functions

After summation over helicity indices, the overlaps of the photon and vector meson wave functions that appear in eqs.(1) and (3) are given by

$$\begin{aligned} & \rho_{\gamma^* V, \pm 1; BSW}(Q^2; z, r) \\ &= \hat{e}_V \frac{\sqrt{6\alpha}}{2\pi} \left( \epsilon_f \omega^2 r [z^2 + \bar{z}^2] K_1(\epsilon_f r) + m_f^2 K_0(\epsilon_f r) \right) \phi_{BSW}(z, r) \\ &\equiv \hat{e}_V \hat{\rho}_{\gamma^*, \pm 1; BSW}(Q^2; z, r) \end{aligned} \quad (12)$$

and

$$\begin{aligned} & \rho_{\gamma^* V, \pm 1; BL}(Q^2; z, r) = \hat{e}_V \frac{\sqrt{6\alpha}}{2\pi} \times \\ & \left( 4\epsilon_f \omega^2 r z \bar{z} [z^2 + \bar{z}^2] K_1(\epsilon_f r) + m_f^2 K_0(\epsilon_f r) \right) \phi_{BL}(z, r) \\ &\equiv \hat{e}_V \hat{\rho}_{\gamma^*, \pm 1; BL}(Q^2; z, r) \end{aligned} \quad (13)$$

for the transverse case, BSW and BL wave functions respectively. For the longitudinal case we can write jointly

$$\begin{aligned} & \rho_{\gamma^* V, 0; X}(Q^2; z, r) = -16\hat{e}_V \frac{\sqrt{3\alpha}}{2\pi} \omega z^2 \bar{z}^2 Q K_0(\epsilon_f r) \phi_X(z, r) \\ &\equiv \hat{e}_V \hat{\rho}_{\gamma^*, 0; X}(Q^2; z, r), \end{aligned} \quad (14)$$

where  $X$  stands for BSW or BL.

## II. OVERLAP STRENGTHS

Previous work [3] has shown the importance for elastic electroproduction processes of the quantities called overlap strengths, formed by integration over the internal variables of the quark-antiquark pairs of the overlap function multiplied by  $r^2$ , written

$$\begin{aligned} Y_{\gamma^* V, T; X}(Q^2) &= \int_0^1 dz \int d^2\mathbf{r} r^2 \rho_{\gamma^* V, \pm 1; X}(Q^2; z, r) \\ &\equiv \hat{e}_V \hat{Y}_{\gamma^* V, T; X}(Q^2), \end{aligned} \quad (15)$$

$$\begin{aligned} Y_{\gamma^* V, L; X}(Q^2) &= \int_0^1 dz \int d^2\mathbf{r} r^2 \rho_{\gamma^* V, 0; X}(Q^2; z, r) \\ &\equiv \hat{e}_V \hat{Y}_{\gamma^* V, L; X}(Q^2) \end{aligned} \quad (16)$$

with  $X$  for BSW or BL. These quantities appear as independent factors in the amplitude, containing all its dependence on  $Q^2$  and on the vector meson and quark masses, whenever the range of the overlap region is small compared to the typical range of the nonperturbative interaction governing the process. This simplification occurs when  $Q^2 + M_V^2 \gtrsim 10 \text{ GeV}^2$ , which means always in  $J/\psi$  and  $\Upsilon$  production, and  $Q^2 \gtrsim 10 \text{ GeV}^2$  in  $\rho, \omega$  and  $\phi$  electroproduction.

The sums of transverse and longitudinal squared strengths for all vector mesons are shown in Fig. 1. Using the variable  $Q^2 + M_V^2$ , where  $M_V$  is the mass of the corresponding vector meson, and extracting factors given by the effective squares of the quark pair charges ( $\hat{e}_V^2 = 1/2, 1/18, 1/9, 4/9$  and  $1/9$  for the  $\rho, \omega, \phi, \psi$  and  $\Upsilon$  mesons respectively), universalities observed in the experimental data are exhibited.

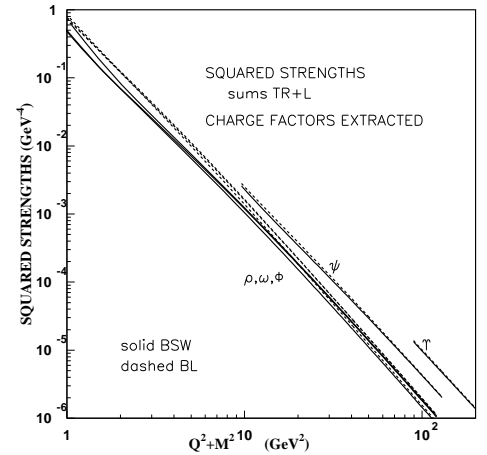


FIG. 1: Sums of transverse and longitudinal squared strengths with extraction of charge factors  $\hat{e}_V^2$ , as functions of  $Q^2 + M_V^2$ . These quantities give all  $Q^2$  dependence of the integrated elastic cross sections. Due to the nearly linear behaviour in the log-log scale, the sums of squared strengths can be parametrized with forms  $A/(Q^2 + M_V^2)^n$ .

The  $Q^2$  dependence of the squared strengths can be represented by

$$\begin{aligned} \hat{Y}_{\gamma^* V, T}^2(Q^2) &= \frac{A_T}{(1 + Q^2/M_V^2)^{n_T}}, \\ \hat{Y}_{\gamma^* V, L}^2(Q^2) &= \frac{A_L(Q^2/M_V^2)}{(1 + Q^2/M_V^2)^{n_L}}, \end{aligned} \quad (17)$$

with the values of  $A_T, n_T, A_L$  and  $n_L$  given in Table III. The use of the numerical values  $M_V^2$  of the vector mesons masses in these parametrizations is inspired in the Vector Dominance Model, with  $n_T = 2$  corresponding to the vector meson propagator. The parametrization is successful in the description of data (in rather limited  $Q^2$  intervals), and can be improved in the light vector mesons cases with  $M$  left as a free parameter

TABLE III: Parameters  $A_T$ ,  $n_T$ ,  $A_L$  and  $n_L$  of eqs. (17) for the squared overlap strengths  $\hat{Y}^2$  in  $\text{GeV}^{-4}$ , directly related to the cross sections.

	BSW			
	transverse		longitudinal	
	$A_{T/L}$	$n_{T/L}$	$A_{T/L}$	$n_{T/L}$
$\rho$	2.18	3.16	0.58	3.38
$\omega$	2.11	3.23	0.74	3.50
$\phi$	0.57	3.27	0.23	3.49
$J/\psi$	$0.26E(-2)$	3.48	$0.19E(-2)$	3.63
$\Upsilon$	$1.33E(-5)$	3.68	$1.14E(-5)$	3.73
	BL			
	transverse		longitudinal	
	$A_{T/L}$	$n_{T/L}$	$A_{T/L}$	$n_{T/L}$
$\rho$	4.46	3.35	0.84	3.42
$\omega$	4.63	3.45	1.04	3.54
$\phi$	1.08	3.47	0.32	3.53
$J/\psi$	$0.30E(-2)$	3.51	$0.21E(-2)$	3.66
$\Upsilon$	$1.39E(-5)$	3.68	$1.18E(-5)$	3.73

(fitting results recommend increases by up to 30 percent in  $M_V$ ). However differences are small and not important at the moment, in view of the limited data. In any case, the reason for the appealing and efficient parametrizations of the form  $1/(Q^2 + M_V^2)^n$  is not understood.

Figure 2 shows the ratios of squared strengths of the longitudinal and transverse cases, for the different vector mesons. According to the factorization property, these quantities correspond to the ratios of longitudinal and transverse cross sections, which are observed experimentally. For light vector mesons ( $\rho, \omega, \phi$ ) the value of  $Q^2$  must be large enough, namely  $Q^2 + M_V^2 \gtrsim 20 \text{ GeV}^2$  and we observe that for these mesons the BSW and BL wave functions show different behaviour in the  $Q^2$  dependence.

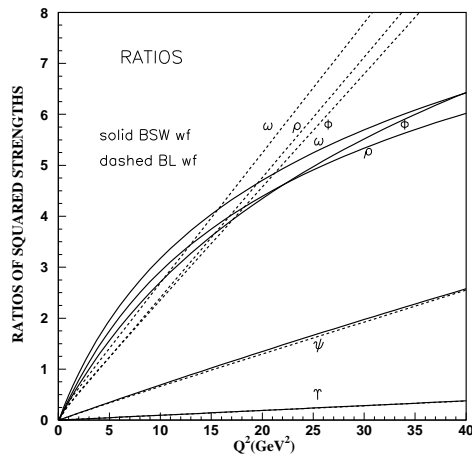


FIG. 2: Ratios of longitudinal to transverse squared strengths, for different vector mesons. In the cases of light vector mesons ( $\rho, \omega, \phi$ ) the BSW and BL wave functions show different behaviour in the  $Q^2$  dependence.

### III. EXPERIMENTAL DATA

The factorization property means that we may write

$$T_{\gamma^* p \rightarrow V p, T/L}(s, t; Q^2) \approx (-2is) G(t) Y_{\gamma^* V, T/L; X}(Q^2) \quad (18)$$

with  $Y$  given by eqs. (15),(16).  $G(t)$  depends on the specific framework and model for the dipole-dipole interaction and on the proton wave function. Depending on the dynamical structure of the model, it may also contain energy dependence due to the dipole-dipole interaction.

The energy dependence in our calculation follows the two-pomeron model of Donnachie and Landshoff [9]. The small dipoles couple through the hard pomeron with energy dependence  $(s/s_0)^{0.42}$ , while large dipoles follows the soft pomeron energy dependence  $(s/s_0)^{0.0808}$ . The reference energy is  $s_0 = (20 \text{ GeV})^2$ .

All observables of differential and integrated elastic cross for the processes of photo and electroproduction of  $J/\psi$  and  $\Upsilon$  vector mesons [1–3] have been calculated using these expressions using the Model of the Stochastic Vacuum (MSV). In Fig. 3 we show the  $Q^2$  dependence of the elastic electroproduction cross section for  $\gamma^* p \rightarrow \psi p$  obtained before [3]. The data are from HERA-ZEUS [27] and HERA-H1 [28]. The line corresponds to the squared overlap strength multiplied by a constant fixed by universal QCD quantities.

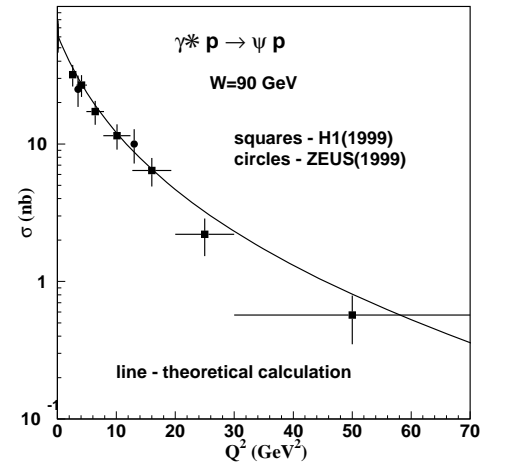


FIG. 3: Integrated elastic cross section for  $J/\psi$  electroproduction as function of  $Q^2$ . Data from [27] (circles) and [28] (squares). The line goes with the squared overlap strength, multiplied by a single constant determined without free parameter using the stochastic vacuum model [3].

These calculations have shown a property of factorization of the amplitudes, with all  $Q^2$  dependence, and all properties specifically dependent on the vector meson structure, described by the quantity called overlap strength, which is the integral over the dipole variables  $r$  and  $z$ , with a weight  $r^2$ , of the photon-meson overlap function.

The comparison with data demonstrates the contents of information concentrated in the wave function overlaps. The

message is that details of proton structure functions are not visible in the kinematical conditions where the nonperturbative method has a full control of the elastic electroproduction process.

Figure 4 shows data of elastic  $\rho$  electroproduction, from Zeus [27] and H1 [29] at energies  $W = \sqrt{s} = 75 - 90 \text{ GeV}$ . The solid line is the overlap strength squared, multiplied by a fixed number  $C = 74 \times 10^3$  converting the squared strengths in  $\text{GeV}^{-4}$  to the cross section in  $\text{nb}$ . The figure shows that the  $Q^2$  dependence of the data above  $Q^2 = 10 \text{ GeV}^2$  is well represented by the overlap of photon and  $\rho$  meson wave functions, with a discrepancy between full MSV calculation and factorized form appearing for smaller  $Q^2$  values.

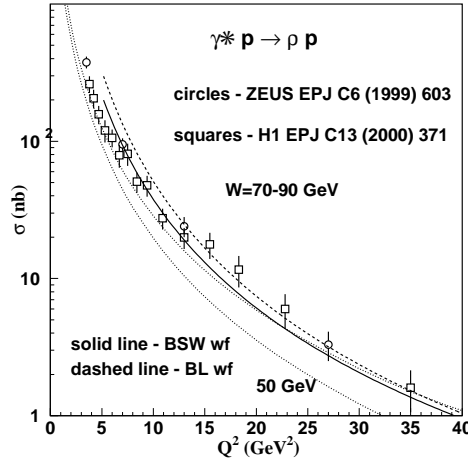


FIG. 4: Integrated elastic cross section for  $\rho$  electroproduction as a function of  $Q^2$ . Data from Zeus [27] (empty circles) and H1 [29] (empty squares) in the energy range 70-90 GeV. The dotted lines show results from the full MSV calculation (not using factorization) with BSW at 50 and 90 GeV to exemplify the energy dependence.

Figure 5 shows the cross sections for  $\rho$ ,  $\psi$  and  $\Upsilon$  electroproduction, reduced by the charge factors  $1/2$ ,  $4/9$  and  $1/9$  respectively, plotted against the variables  $Q^2 + M_V^2$ . The  $\psi$  and  $\rho$  data and theoretical lines are the same as in Figs. 3 and 4. The  $\Upsilon$  photoproduction data (triangles) from ZEUS [30] and H1 [31] at about  $W=100 \text{ GeV}$  are compared to the theoretical calculation at this energy [2].

The plot exhibits the partial universality of the data in terms of the variables  $Q^2 + M_V^2$ , showing that the shifts observed experimentally between the heavy and light mesons are theoretically reproduced as natural consequences of the construction of the overlap of photon and meson wave functions.

Our construction of the wave functions uses the experimental decay rates of the vector mesons, which effectively incorporate QCD corrections, and thus makes phenomenologically realistic representations of the vector meson structures. We may conjecture that the shifts observed in plots of data and of squared strengths are due to QCD corrections of the decay rates, which specifically depend on the quark masses, and thus are different for the different mesons. It will be interesting to see their influence on the parameters of wave functions that

are used for the evaluation of electroproduction, in order to investigate a possible origin of the observed shifts.

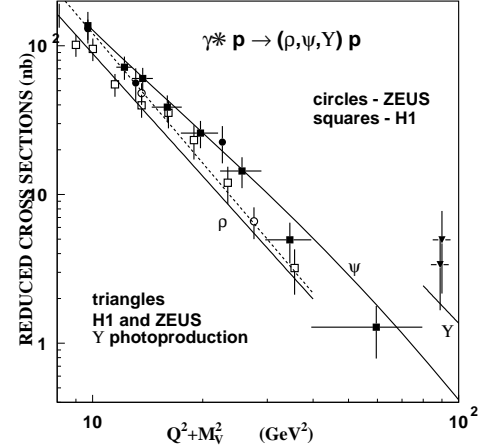


FIG. 5: Integrated elastic cross section for  $J/\psi$  [27, 28] and  $\rho$  electroproduction [27, 29], and for  $\Upsilon$  photoproduction [30, 31]. The lines represent the theoretical calculations explained in the text. For  $J/\psi$  and  $\Upsilon$  the differences between the two kinds of vector meson wave function are not important, as shown in Fig. 2. For  $\rho$  the differences are illustrated by the dashed line corresponding to BL.

Figure 6 shows the experimental ratio [27, 29, 32, 33] between longitudinal and transverse cross sections in  $\rho$  electroproduction, compared to the ratio of longitudinal to transverse squared overlap strengths. In the ratio, the specific dynamics of the process of interaction of the  $q - \bar{q}$  dipoles with the proton cancels out, so that a clear view is obtained of the self-contained role of the photon-meson wave function overlap. The comparison is to be taken more seriously for  $Q^2 \gtrsim 10 \text{ GeV}^2$ . The cross section with transverse polarization falls to zero much more quickly, and the ratio  $R = \sigma(L)/\sigma(T)$  becomes sensitive to the helicity structure of the wave function. Thus the predictions for the ratio  $R$  given by the BSW and BL wave functions, in the light meson cases, are very different. This is obviously an area that deserves exploration, both experimentally and theoretically.

#### IV. CONCLUSIONS

The results discussed in this paper are consequences of the form of the amplitude in eqs. (1),(2),(3) written as integrations over configuration space coordinates. The fundamental quantity in the calculations is the dipole-dipole interaction, which in nonperturbative language takes the form of loop-loop correlation in QCD vacuum. The dipoles appear in the  $\gamma^* - V$  transition (overlap of the wave functions) and in the proton structure. The treatment is typical of soft QCD calculation, and provides very successful phenomenology of pp and hadron-hadron scattering [6]. Different models must provide the quantities relating the amplitudes with the overlap strengths, written in terms of their basic ingredients and parameters. We particularly use the Stochastic Vacuum Model to

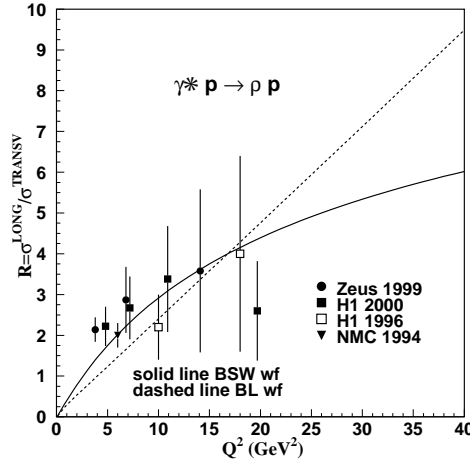


FIG. 6: Ratio of polarized cross sections in  $\rho$  electroproduction. Data from [27, 29, 32, 33]. The lines represent ratios of overlap strengths, showing different behaviour for BSW and BL wavefunctions.

produce measured quantities, but the factorization property is more general.

In the treatment of  $J/\psi$  electroproduction we have shown that, where the range of the overlap function is small compared to the proton size and to the range of correlation func-

tions of the QCD vacuum, a factorization of the amplitude takes place [3], such that the  $Q^2$  dependence of observables is fully described in terms of the overlap strengths of eqs.15. For heavy, small sized vector mesons (such as  $J/\psi$ ), factorization of the amplitude occurs even in photoproduction processes. For the light vector mesons, of broader wave functions and broader overlaps with the photon when  $Q^2$  is small, the factorization holds clearly only for large values of  $Q^2$ . In  $\rho$  electroproduction this means  $Q^2 \gtrsim 10 \text{ GeV}^2$ .

Comparing our results with experimental data on cross sections for  $J/\psi$  and  $\rho$  electroproduction plotted against  $Q^2 + M_V^2$  in Fig. 5, we show the approximate universal behaviour of different mesons, with the shift that has been observed experimentally and is here quantitatively predicted by the overlap strength.

#### Acknowledgments

The authors are grateful to H. G. Dosch for participating in several aspects of the present work, and wish to thank DAAD(Germany), CNPq(Brazil), and FAPERJ(Brazil) for support of the scientific collaboration program between Heidelberg and Rio de Janeiro groups working on hadronic physics.

- 
- [1] H.G. Dosch, T. Gousset, G. Kulzinger, and J.J. Pirner, Phys. Rev. D **55**, 2602 (1997).
  - [2] H.G. Dosch and E. Ferreira, Eur. Phys. J. C **29**, 45 (2003).
  - [3] H.G. Dosch and E. Ferreira, Phys. Lett. B **576**, 83 (2003).
  - [4] H.G. Dosch, Phys. Lett. B **190**, 177 (1987).
  - [5] H.G. Dosch and Y.A. Simonov, Phys. Lett. B **205**, 339 (1988).
  - [6] H.G. Dosch, E. Ferreira, and A. Kramer, Phys. Rev. D **50**, 1992 (1994).
  - [7] O. Nachtmann, Ann. Phys. **209**, 436 (1991).
  - [8] E. Ferreira and V.L. Baltar, Nucl. Phys. A **748**, 608 (2005).
  - [9] A. Donnachie and P.V. Landshoff, Phys. Lett. B **437**, 408 (1998).
  - [10] A. Donnachie and H. G. Dosch, Phys. Rev. D **65**, 014019 (2002).
  - [11] S.J. Brodsky, L. Frankfurt, J.F. Gunion, A.H. Mueller, and M. Strikman, Phys. Rev. D **50**, 3134 (1994).
  - [12] A.H. Mueller, Nucl. Phys. B **415**, 373 (1994).
  - [13] A.D. Martin, M.G. Ryskyn, and T. Teubner, Phys. Rev. D **62**, 014022 (2000).
  - [14] A.H. Mueller, Nucl. Phys. B **643**, 501 (2002).
  - [15] P.A.M. Dirac, Rev. Mod. Phys. **21**, 392 (1949).
  - [16] J.B. Kogut and D. E. Soper, Phys. Rev. D **1**, 2910 (1970); J.D. Bjorken, J.B. Kogut, and D.E. Soper, Phys. Rev. D **3**, 1382 (1971).
  - [17] J. Kogut, L. Susskind, Phys. Rep. **8**, 75 (1973).
  - [18] G.P. Lepage and S.J. Brodsky, Phys. Rev. D **22**, 2157 (1980).
  - [19] G.P. Lepage *et al.*, in *Particles and Fields 2*, Proceedings of the Banff Summer Institute, Banff, Canada, 1981, edited by A.Z. Capri and A.N. Kamal (Plenum, New York, 1983).
  - [20] S.J. Brodsky, H.C. Pauli, and S.S. Pinsky, Phys. Rep. **301**, 299 (1998).
  - [21] N. N. Nikolaev and B. G. Zakharov, Z. Phys. C **49**, 607 (1991).
  - [22] A. C. Caldwell and M. A. Soares, Nucl. Phys. A **696**, 125 (2001).
  - [23] M. Wirbel, B. Stech, and M. Bauer, Z. Phys. C **29**, 637 (1985); M. Bauer, B. Stech, and M. Wirbel, Z. Phys. C **34**, 103 (1987).
  - [24] S. Eidelman *et al.*, Phys. Lett. B **592**, (2004) and updates in <http://pdg.lbl.gov>.
  - [25] J. Nemchik, N.N. Nikolaev, and B.G. Zakharov, Phys. Lett. B **341**, 228 (1994); J. Nemchik, N.N. Nikolaev, E. Predazzi, and B.G. Zakharov, Z. Phys. C **75**, 71 (1997).
  - [26] S. Munier, A.M. Staśto, and A.H. Mueller, Nucl. Phys. B **603**, 427 (2001).
  - [27] J. Breitweg *et al.*, Zeus Coll., Eur. Phys. J. C **6**, 603 (1999).
  - [28] C. Adloff *et al.*, H1 Coll. Eur. Phys. J. C **10**, 373 (1999).
  - [29] C. Adloff *et al.*, H1 Coll. Eur. Phys. J. C **13**, 371 (2000).
  - [30] J. Breitweg *et al.*, Zeus Coll., Phys. Lett. B **437**, 432 (1998).
  - [31] C. Adloff *et al.*, H1 Coll. Phys. Lett. B **483**, 23 (2000).
  - [32] S. Aid *et al.*, H1 Coll., Nucl. Phys. B **468**, 3 (1996).
  - [33] M. Arneodo *et al.*, NMC Coll., Nucl. Phys. B **429**, 503 (1994); P. Amaudruz *et al.*, Zeit. Phys. C **54**, 239 (1992).
  - [34] J. Breitweg *et al.*, Zeus Coll. Eur. Phys. J. C **12**, 393 (2000).
  - [35] S. Chekanov *et al.*, ZEUS Coll., Nucl. Phys. B **695**, 3 (2004).